DOE/NASA/0247-2
NASA CR-174982
PPI-FID-300102

IN - 32894

WEST-3 Wind Turbine Simulator Development

Volume 2: Verification

S. Sridhar
Paragon Pacific Inc.

July 1985

(NASA-CR-174982) WEST-3 WIND TURBINE SIMULATOR DEVELCPMENT. VOLUME 2: VERIFICATION Final Report (Paragon Pacific, Inc.) 31 p CSCL 10A
N87-10531
Unclas
G3/44 44357

Prepared for
NATIONAL AERONAUTICS AND SPACE ADMINISTRATION
Lewis Research Center
Under Contract DEN 3-247

for
U.S. DEPARTMENT OF ENERGY
Conservation and Renewable Energy
Wind/Ocean Technology Division

Printed in the United States of America

Available from
National Technical Information Service
U.S. Department of Commerce
5285 Port Royal Road
Springfield, VA 22161

NTIS price codes[1]
Printed copy: A03
Microfiche copy: A01

[1]Codes are used for pricing all publications. The code is determined by the number of pages in the publication. Information pertaining to the pricing codes can be found in the current issues of the following publications, which are generally available in most libraries: *Energy Research Abstracts (ERA); Government Reports Announcements* and Index (*GRA* and I); *Scientific and Technical Abstract Reports (STAR);* and publication, NTIS-PR-360 available from NTIS at the above address.

DOE/NASA/0247-2
NASA CR-174982
PPI-FID-300102

WEST-3 Wind Turbine Simulator Development

Volume 2: Verification

S. Sridhar
Paragon Pacific Inc.
Torrance, California 90503

July 1985

Prepared for
National Aeronautics and Space Administration
Lewis Research Center
Cleveland, Ohio 44135
Under Contract DEN 3-247

for
U.S. DEPARTMENT OF ENERGY
Conservation and Renewable Energy
Wind/Ocean Technology Division
Washington, D.C. 20545
Under Interagency Agreement DE-AI01-76ET20320

CONTENTS

PRECEDING PAGE BLANK NOT FILMED

FOREWORD

The work documented in this report was sponsored by the NASA Lewis Research Center, under Contract DEN3-247. The work was performed by Paragon Pacific Inc., 530 Maple Ave., Torrance, CA 90503, during the final phase of the contract. The NASA Project Manager was Mr. D. C. Janetzke.

Principal participants in the contract activity were J. A. Hoffman, D. Weisz and S. Sridhar of Paragon Pacific Inc., and Dr. M. D. Campbell of Talisman Systems, Drawer CP255, Manhattan Beach, CA 90266.

The assistance of Mr. G. K. Ellis of Sverdrup Technology Inc. on contract to NASA Lewis Research Center during the verification studies is gratefully acknowledged.

SUMMARY

The details of a study to validate WEST-3, a new real time wind turbine simulator developed by Paragon Pacific Inc., are presented in this report. For the validation, the MOD-0 wind turbine was simulated on WEST-3. The simulation results were compared with those obtained from previous MOD-0 simulations, and with test data measured during MOD-0 operations. The study was successful in achieving the major objective of proving that WEST-3 yields results which can be used to support a wind turbine development process.

The blade bending moments, peak and cyclic, from WEST-3 are shown to correlate reasonably well with the available MOD-0 data. The WEST-3 is shown to be a significant improvement over the previous WEST systems as evidenced by the better correlations of the blade bending moments with test data, and its ability to predict the resonance phenomena observed during MOD-0 operations.

Also presented in the report is a description of a numerical instabilty problem caused by the coupling of the rotor and the power train models. Though an ad hoc solution to the problem was found, it is pointed out that a more general and systematic approach must be found for solving the problem of instabilities arising out of the coupling of two or more simulation models.

The results of the study indicate that some parts of the existing WEST-3 simulation model may have to be refined for future work; specifically, the aerodynamics, and the procedure used to couple the rotor model with the tower and the power train models.

1. INTRODUCTION

Paragon Pacific Inc. has developed WEST-3 for the real time simulation of wind turbines. WEST-3 is an all digital, fully programmable, parallel processing system. The wind turbine simulation model implemented in WEST-3 has the following features:

1. Three elastic degrees of freedom for each blade
2. Tower model with six physical degrees of freedom
3. Power train model with two degrees of freedom
4. Blade tip loss model for the rotor
5. Tower shadow model without "aliasing" effects
6. Gimballed rotor capability
7. Nonlinear wind shear model
8. Bandpass wind gust filters

It should be noted that the modular nature of the simulation model makes it very easy to introduce changes in the model; for example, a new control system or power train model.

The MOD-0 wind turbine simulation model was chosen for validating WEST-3. The model has two elastic degrees of freedom, one flatwise and one edgewise, for each blade. The tower is represented by three elastic degrees of freedom, surge, sway, and yaw (torsion of the tower). The control system provides for servo control of the output power and the rotor speed by changing the blade pitch angle. Descriptions of the MOD-0 simulation model can be found in References 1 and 2.

Presented in this report are the details of the WEST-3 validation study. The WEST-3 simulation results were compared to those obtained from the WEST-2 simulator (Reference 3), the wind energy version of the Modular Stability Derivative (MOSTAB) computer program (References 4 and 5), and the MOD-0 test data measured on the experimental machine in operation at NASA's Plum Brook Station near Sandusky, Ohio (Reference 6).

The validation exercise was sucessful in achieving the major objective: proving that WEST-3 yields useful results which can be used to support a wind turbine development process. Additionally, the study was useful in identifying a potential source of numerical instability in the simulation of complex systems such as wind turbines.

The MOD-0 data cases (operating conditions), used in the study, and the specific validation tasks are defined in Section 2. A description of the numerical instability problem encountered during the study is presented in Section 3. The results of the validation are given in Section 4, along with a discussion of the results. Some concluding remarks can be found in Section 5.

2. VALIDATION CASES AND TASKS

For the MOD-0 wind turbine, two sets of reference test data are available (Reference 6). The data sets have been designated as MOD-0 data Cases I and IV. The operating conditions corresponding to these cases are as follows:

	Case I	Case IV
Power Output, kw	100	100
Rotor Speed, rpm	40	40
Wind Speed, mph	25	28
Wind Direction; angle with rotor axis, degrees	4	12
Wind Shear, per cent	15	15
Tower Shadow Strength, per cent	50	28
Tower Shadow Sector, degrees	30	30
Yaw Drive	single	locked
Yaw Drive stiffness, ft-lb/rad	7.91×10^{6}	1.0×10^{12}

The wind direction angle defines the cross wind component. The wind shear variation is assumed to be linear with altitude, varying from +15 percent of the nominal wind speed at the top of the rotor disk to -15 percent at the bottom of the disk. In Case I, a staircase inside the tower produced a strong tower shadow estimated to be 50 percent, i.e., wind speed is reduced by 50 percent behind the tower.

The test data sets contain time histories and harmonic analyses of blade bending moments along with other data such as tower deflections and shaft loads. For the WEST-3 validation, only the blade bending moment data was used for the comparisons, as specified in Reference 7. The following tasks were performed during the study:

1. Comparisons of the blade #1 bending moments (flatwise and edgewise) at station 40 (5 per cent span) and station 370 (49 per cent span). The WEST-3 results were compared with test data and MOSTAB results.

2. Harmonic analysis of the blade bending moments.

3. Variation of the yaw drive stiffness; the objective was to confirm the ability of the simulation model to predict the resonances observed during MOD-0 operations.

4. A numerical instability problem was investigated, details of which are presented in the next section.

3. NUMERICAL INSTABILITY PROBLEM

During the validation study, a severe numerical instability problem was encountered. Presented here are the details of the effort to identify, understand and correct the instability.

3.1 Nature of the Instability

Each of the subsystems in the simulation model was checked separately for correctness, and then coupled together to form the full model. For a complex system, such a procedure is perhaps the best way to implement a simulation. In the case of the MOD-0 simulation on WEST-3, running of the full model indicated that there was a severe instability problem.

Identification of the precise nature of the problem was in itself a nontrivial task, calling for a careful interpretation of the output of WEST-3 before the instability occured; in this case at about 200 milliseconds from the start. It was established that the coupling of the rotor and power train models was the cause of the problem.

Here, for clarity, simplified models of the rotor and the power train are used to explain the observed phenomenon. The relevant scalar equations of motion, for a fixed blade pitch angle, can be written as

Rotor Model:

$$\ddot{q} + 2\,c\,w\,\dot{q} + w^2\,q = G - K_1\,\dot{z}$$

$$M_H = M_o - J_R\,\dot{z} - K_2\,\ddot{q}$$

Power Train Model:

$$J_H\,\dot{z} = -\,M_p + M_H$$

where an overdot denotes a time derivative, and the following nomenclature has been used:

q	edgewise modal coordinate
w	natural frequency of the edgewise mode
c	damping factor
G	generalized modal excitation
z	rotor speed
M_o	moment due to external forces
M_H	hub moment transmitted to the power train
J_R	rotor inertia
J_H	hub inertia
M_p	resisting moment from the power train
K_1	constant (function of the edgewise modal data)
K_2	constant (function of the edgewise modal data)

Ideally, for an exact solution, one would first solve the equations simultaneously for the accelerations, $\ddot{q}$ and $\dot{z}$ (i.e., eliminate the hub moment M_H), and then perform the numerical integrations. For a number of valid reasons, such as improving the simulation speed, the equations in WEST-3 are solved in the following sequence: the modal acceleration $\ddot{q}$, and the hub moment M_H are computed in the rotor model by using the rotor acceleration $\dot{z}$ computed in the previous time step by the power train model. The hub moment is then fed into the power train model for computing a new rotor acceleration. The procedure is shown schematically in Figures 1 and 2. The numbers shown in Figure 2 are all scaled and normalized numbers and correspond to those used in WEST-3.

Such a procedure for coupling two models is frequently used in high speed simulation, and is fully acceptable in many cases. However, in the case of the rotor - power train coupling, the result is a severe instability for the following reasons.

1. There is a relatively high gain in the power train forward loop ($1/J_H$), because the hub inertia J_H is a small fraction of the rotor inertia J_R.

2. The rotor model uses the rotor acceleration computed in the previous time step, i.e., there is a transport delay in the system as shown in Figure 2.

3. The edgewise mode is very lightly damped.

The character of the violent instability, shown qualitatively in Figure 3, is essentially a divergence at the frequency of numerical integration. Such an instabilty problem cannot be solved by reducing the integration step size and/or by using sophisticated multi-pass numerical integration algorithms.

In previous WEST simulations, which did not include the edgewise mode, the problem was solved by rewriting the power train equation as,

$$(J_H + J_R)\ \dot{z} = -\ M_P + M_H + J_R\ \dot{z}$$

thus eliminating the high gain in the power train forward loop. The corresponding modification to the block diagram is shown in Figure 4. Note that the J_R loops of Figures 2 an 4 cancel each other. For the WEST-3, this modification failed to solve the problem; the result is shown in Figure 5. The instability, which is distinctly different from that shown in Figure 3, is a reflection of the presence of the lightly damped blade edgewise mode. The results of Figure 5 were confirmed by a detailed analysis of the system in the frequency domain via Bode plots.

3.2 Solution to the Instability Problem

It should be emphasized that the observed instability is not inherent to the physics of the problem, and is only a consequence of the method used to solve the equations of motion (see Figure 3). This can be easily demonstrated by first solving the equations of motion simultaneously for the accelerations q and Z (i.e., eliminating hub moment M_H), and then performing the numerical integrations. Unfortunately, the equivalent of such approach for the WEST-3 simulation model would require an extensive reformulation of the model. Cost and schedules precluded such a reformulation effort.

Thus, what was needed was a procedure to extract the exact solution from the existing computations in the WEST-3 simulation model, without resorting to an extensive reformulation of the model. Such a procedure was devised, and is presented in the following (using the simplified equations).

The governing equations can be rewritten as,

$$\ddot{q} = \ddot{q}_1 + \ddot{q}_2 \; ; \qquad \ddot{q}_1 = - 2 c w \dot{q} - w^2 q + G - K_1 \dot{z}_{old},$$

$$q_2 = - K_1 (\dot{z} - \dot{z}_{old})$$

$$M_H = M_1 + M_2 \; ; \qquad M_1 = M_o - J_R \dot{z}_{old} - K_2 \ddot{q}_1,$$

$$M_2 = - J_R (\dot{z} - \dot{z}_{old}) - K_2 \ddot{q}_2$$

$$J_H (\dot{z} - \dot{z}_{old}) = - M_p + M_H - J_H \dot{z}_{old}$$

In the equations given above, the quantities with a "1" subscript correspond to those which are being computed in the WEST-3 simulation model. The idea is to compute the quantities M_2 and $\ddot{q}_2$ so that the exact solution can be recovered. It can be shown, after some algebra that,

$$\ddot{q}_2 = - (K_1 / (J_H + J_R - K_1 K_2)) (M_1 - M_p - J_H \dot{z}_{old})$$

$$M_2 = ((J_R/K_1) - K_2) \ddot{q}_2$$

$$z = z_{old} - (1/K_1) \ddot{q}_2$$

The solution procedure is shown schematically in Figure 6. It can be shown that the procedure given above is equivalent to obtaining the the exact solution. The required corrections were incorporated into the WEST-3 simulation model and the instability problem was successfully eliminated.

4. RESULTS AND DISCUSSION

The aeroelastic rotor model is the central piece of a wind turbine simulation model. As such, the validation exercise began with a detailed verification of the results generated by the rotor model. The rotor was set to operate in a steady state under nominal operating conditions; constant speed of 40 rpm, wind speed of 26 mph, and blade pitch angle of -7.4 degrees. There were no asymmetric excitations such as tower shadow and wind shear. Some of the quantities chosen for validation were,

1. Distributed aerodynamic loads along the blade
2. Total thrust and torque
3. Blade root bending moments
4. Changes in the aerodynamic loads due to changes in wind speed
5. Changes in the aerodynamic loads due to changes in blade pitch angle

Not unexpectedly, in this phase of the validation a number of minor errors in the data, and in the implementation of the simulation were identified and corrected. Good agreement was found when the results were compared with those obtained from the MOSTAB computer program and/or hand calculations.

Once the rotor model was validated in the steady state conditions, the full simulation model was assembled by adding in the tower shadow, wind shear, power train, control system and tower models. For the validation exercise, the nominal power output of 100 kw was commanded in to the model by specifying a corresponding generator torque acting on the power train. Coupling of the rotor and power train models caused a severe numerical instability problem, which was corrected as described in Section 3.

During the running of the full simulation model, another discrepancy was observed. To generate the commanded power, the control system was setting the blade pitch angle (nominally around -7.4 degrees) to much higher values, i.e., the rotor was producing excessive torque. The reason was found to be the high damping values used in the power train model. Since these damping values are unlikely to be known to a high degree of precision, they were adjusted to obtain a blade pitch angle of approximately -7.4 degrees.

4.1 Blade Flatwise and Edgewise Bending Moments

The coordinate system in which the blade bending moments are defined is shown in Figure 7. The azimuthal angle is zero degrees when the blade points downward and is in the tower shadow. The flatwise bending moment is positive when the blade bends into the wind, i.e., towards the tower. The edgewise bending moment is positive when the blade leading edge is in tension.

Final results of the WEST-3 validation study are presented as follows: Time histories of the blade flatwise and edgewise bending moments at stations 40 and 370, for Cases I and IV are shown in Figures 8 through 11. Cyclic bending moments at stations 40 and 370, for Cases I and IV are shown in Table 1. Peak bending moments at stations 40 and 370, for Cases I and IV are shown in Table 2. Also shown in Tables 1 and 2 are the results obtained from, the WEST-2 simulator (Reference 3), the MOSTAB computer program, and the test data (Reference 6).

A careful analysis of the WEST-3 results indicates the following:

- The WEST-3 time histories are generally in qualitative agreement with those measured in actual MOD-0 operations (Reference 6). The quantitative correlation is, however, less satisfactory.

- The correlation of the peak and cyclic blade moments with nominal test data is reasonably good. The correlation at station 40 is much better than that at station 370. The WEST-3 cyclic moments are typically higher than nominal test data.

- The WEST-3 results are significantly better than those obtained from WEST-2 (Reference 3).

The discrepancies between the results from WEST-3 and those previously published, clearly indicate that there is scope for improving the simulation model that is presently being used. Specifically,

- The aerodynamic representation being used is relatively simple, and is slated for refinement in future work.

- The present method of coupling the rotor model to the tower and the power train models should be reexamined; the coupling procedure may have to be reformulated.

4.2 Harmonic Analysis

Time histories of the blade bending moments were analyzed for their harmonic content. A simple computer program was used to generate the fourier coefficients. The program accepts as input the time histories of the forces and moments, resolved into rotor axes (Figure 7), at the shaft center line. Other inputs to the program are: blade weight, precone angle, centrifugal tension on the blade, desired radial location along the blade, and the direction (blade pitch angle) along and perpendicular to which the moments are to resolved. Additionally, scale factors for the forces and moments can be input to the program so that the output from WEST-3, for example, from a strip chart recorder, can used for the time histories. A listing of the computer program can be found in Reference 3.

The results of the harmonic analysis along with those obtained from the WEST-2 simulator (Reference 3), and from the test data (Reference 6) are given in Tables 3.

4.3 Variation of Yaw Drive Stiffness

In the MOD-0 wind turbine there is yaw drive mechanism which can be used to align the rotor axis with the wind direction. The yaw drive can be configured to exibit different stiffnesses ranging from zero (i.e., a free condition), to a very high value corresponding to a fixed condition. Test data, and previous studies of the variation of yaw drive stiffness (Reference 1) have indicated the presence of resonances in the blade moments corresponding to frequencies which are 1/2, 1/4, and 1/6 of the rotor's rotational frequency; i.e., 2 per rev, 4 per rev and 6 per rev responses.

During the validation of WEST-2, the simulations did not exibit any resonances with the variation of yaw drive stiffness. This was attributed to the fact that the WEST-2 simulation model did not include the blade edgewise degree of freedom. It has been of considerable interest to establish whether WEST-3, which includes the blade edgewise degree of freedom, exhibits the presence of the resonances.

Initial studies indicated that, at low yaw drive stiffnesses, some of the the tower responses were mildly unstable leading to divergence over an extended period of simulation. The cause was traced to an incorrect handling of the blade mass effects in the coupling of the rotor and tower models. The modal properties for the tower have been generated with an added mass and inertia placed on top of the tower to account for the presence of the pod, rotor, and power train. When the rotor and the tower models are coupled together, the blade mass (whose effects are already accounted for in the rotor model) has to be deleted from the tower model. A correct implemetation of this effect eliminated the observed slow divergence.

For this part of the validation, the operating conditions chosen were, a wind speed of 26 mph and a tower shadow strength of 28 per cent. Figure 12 shows plots of the blade root bending moments, and the tower response (torsional modal accceleration) as functions of the effective yaw drive stiffness. The effective stiffness is the equivalent stiffness of the yaw drive and the tower acting as two springs series. The plot was obtained by using the analog input facilities of WEST-3 to do a very slow sweep of the torsional mode's natural frequency, which is directly correlatable to the effective stiffness of the yaw drive.

Figure 13 shows the cyclic blade moments plotted as functions of the square root of the effective yaw stiffness of the tower. For convenience, the WEST-3 results were superposed on the figure which was taken from Reference 1. The cyclic blade moments for the ten values of the yaw drive stiffness are given in Table 4. Also given in the table are the values of the corresponding effective stiffnesses. Finally, to indicate qualitatively, the harmonic content of the responses at three values of the the yaw drive stiffness, the time histories of the blade moments and the tower response are shown in Figures 14,15 and 16; the three values of the yaw drive stiffnesses correspond to 2/rev, 4/rev and 6/rev responses.

Figures 13 through 16 clearly indicate that the WEST-3 simulation model is able to predict the various resonances observed in MOD-0 operations. Referring to Figure 14, it should be noted that the magnitude of a resonance peak is strongly dependent on the amount of damping acting in the the yaw direction. The value of the damping is not known exactly, so that a precise correlation of the peaks shown in Figure 14 was not expected.

5. CONCLUDING REMARKS

- The WEST-3 simulation system has been validated via the MOD-0 wind turbine simulation model. The major objective of the validation exercise has been met, i.e., proving that WEST-3 yields results which can be used to support a wind turbine development process.

* The MOD-0 simulation results from WEST-3 correlate reasonably well with those obtained from previous simulations, and with measured test data. The discrepancies which do exist are attributable to differences in the various simulation models, as well the inherent problems of accurately modelling a complex system such as a wind turbine; in particular, the aerodynamic phenomenon. There is also scope for improving the existing simulation model. Specifically

    1. The aerodynamic representation used in this study is relatively simple, and is slated for major refinements in future work.

    2. The method of coupling the rotor model to the tower and the power train models needs to be reexamined; reformulation of the presently used procedure may be indicated.

* The WEST-3 system is a significant improvement over the previous WEST sytems as evidenced by the better correlation of the blade bending moments with test data, and its ability to predict the MOD-0 resonance phenomena associated with changes in the yaw drive stiffness.

* The numerical instability encountered during the validation study is generic to the coupling of the simulation models of two components, the severity of the problem being a function of the specific dynamics of the models. Though an ad hoc solution was found during the study, a more general and systematic approach must be found for solving the problem of instabilities arising out of the coupling of simulation models of two or more components.

REFERENCES

1. Kaza, K. R. V., Janetzke, D. C., and Sullivan, T. L., "Evaluation of MOSTAS Computer Code for Predicting Dynamic Loads In Two-Bladed Wind Turbines," DOE/NASA/1028-79/2, NASA TM-79101, 1979.

2. Hoffman, J. A., "Development Report: Wind Energy System Time-domain (WEST) Analyzers Using Hybrid Simulation Techniques," NASA CR-159737, Oct. 1979.

3. Hoffman, J. A., "Verification Study Results: Comparisons Between Analysis Results Produced By The Wind Energy System Time Domian (WEST) Simulator With Those Produced By The MOSTAB Digital Computer Code," PPI-FID-300081, Prepared under NASA Contract DEN3-247, Paragon Pacific Inc., June 1982.

4. Hoffman, J. A., "User's Manual for the Modular Stability Derivative Program - High Frequency Wind Turbine Version (MOSTAB-HFW)," PPI-1014-8, Paragon Pacific Inc., 1977.

5. Hoffman, J. A., "Coupled Dynamic Analysis of Wind Energy Systems," PPI-1014-11, Paragon Pacific Inc., NASA CR-135153, 1977.

6. Spera, D. A., "Comparison of Computer Codes For Calculating Dynamic Loads In Wind Turbines," DOE/NASA/1028-78/16, NASA TM-73773, 1977.

7. Anonymous, Statement of work of NASA Contract DEN3-247 for WEST Improvement and MOSTAS and WEST support Programs, June 1981.

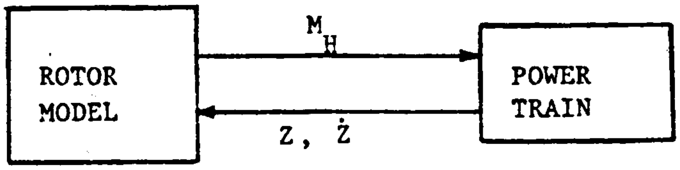

Figure 1. Schematic of Rotor and Power Train Models in WEST-3

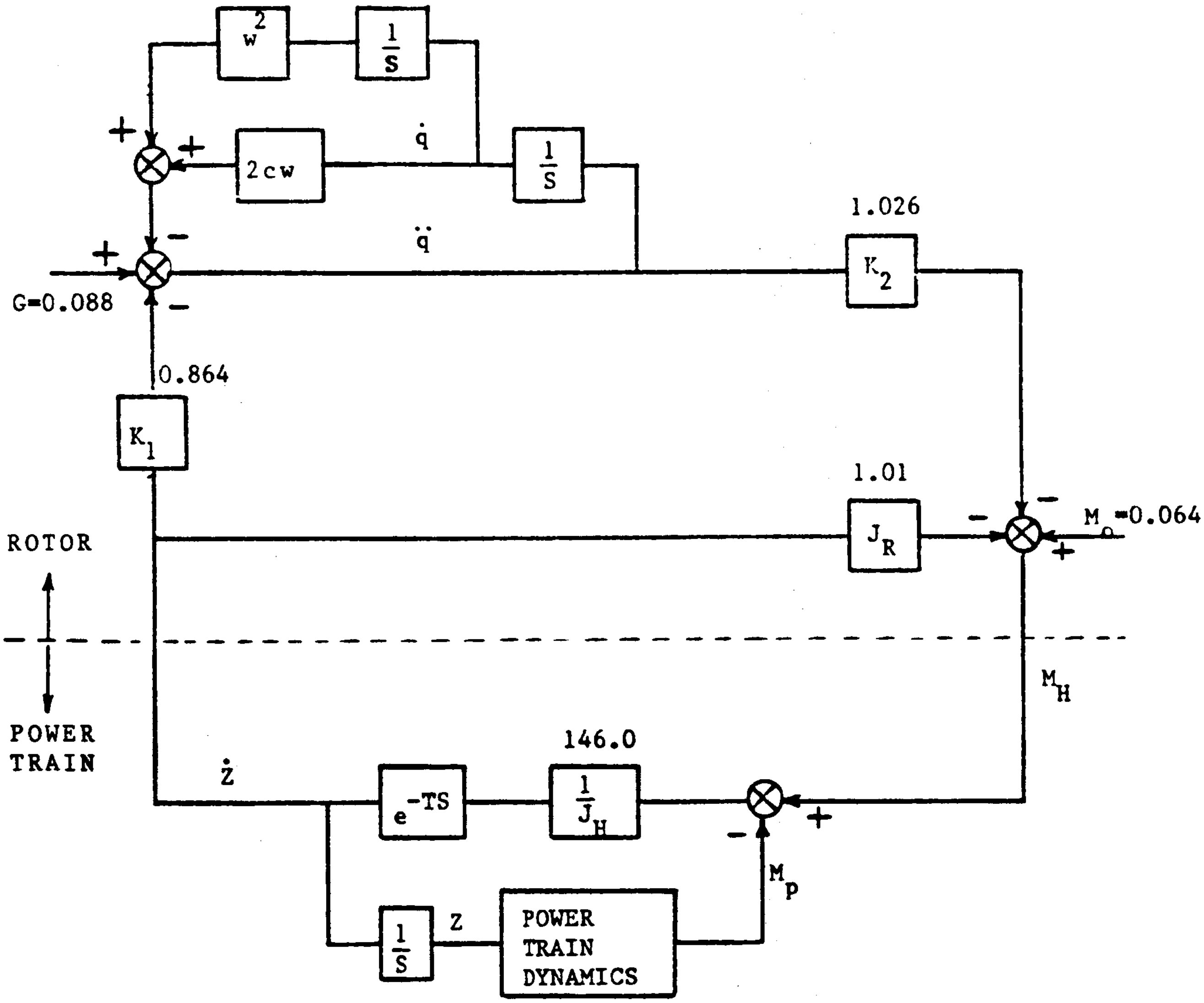

Figure 2. Block Diagram of the Rotor and Power Train Equations

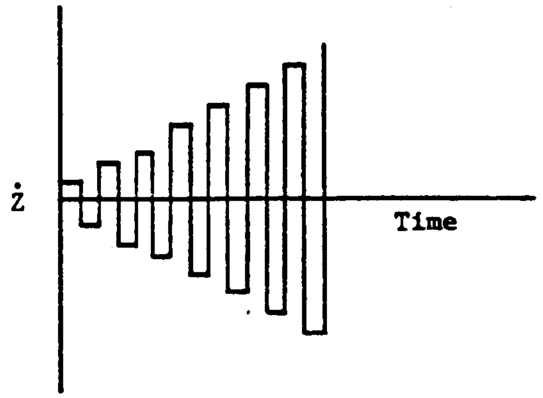

Figure 3. Instability at the Frequency of Numerical Integration

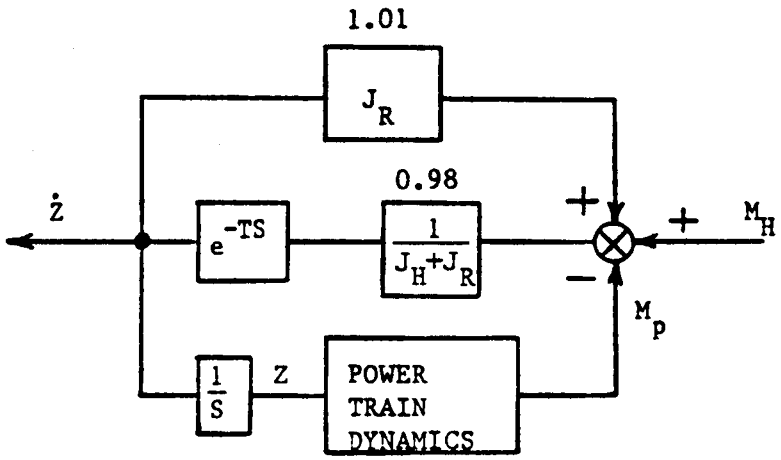

Figure 4. Modification of the Power Train Equation

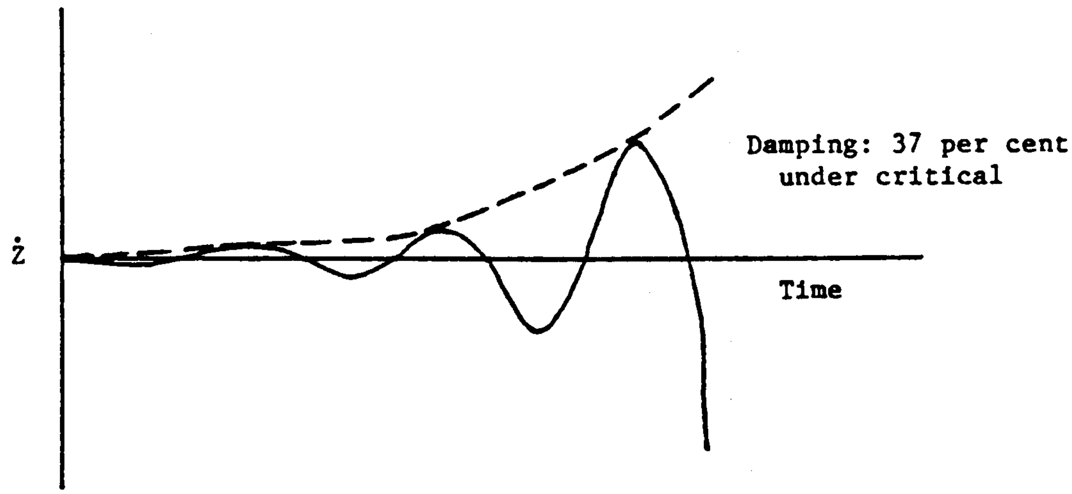

Figure 5. Failure of Modification Shown in Figure 4 to correct the instability

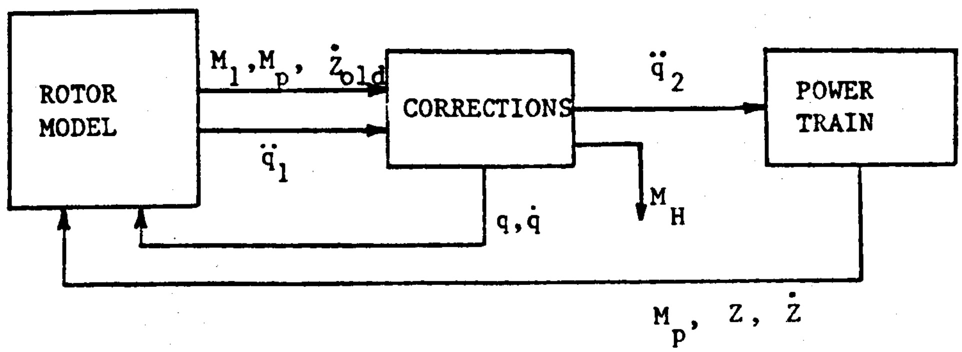

Figure 6. Schematic of the Solution Procedure Devised for the WEST-3 Model

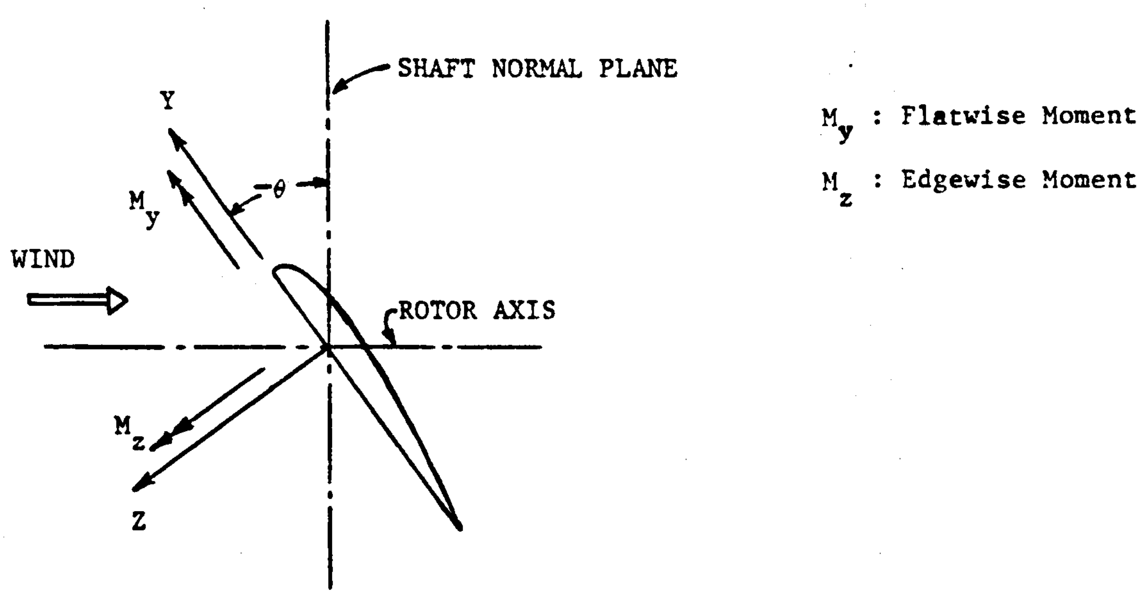

Figure 7. Coordinate System in which the Blade Bending Moments are defined

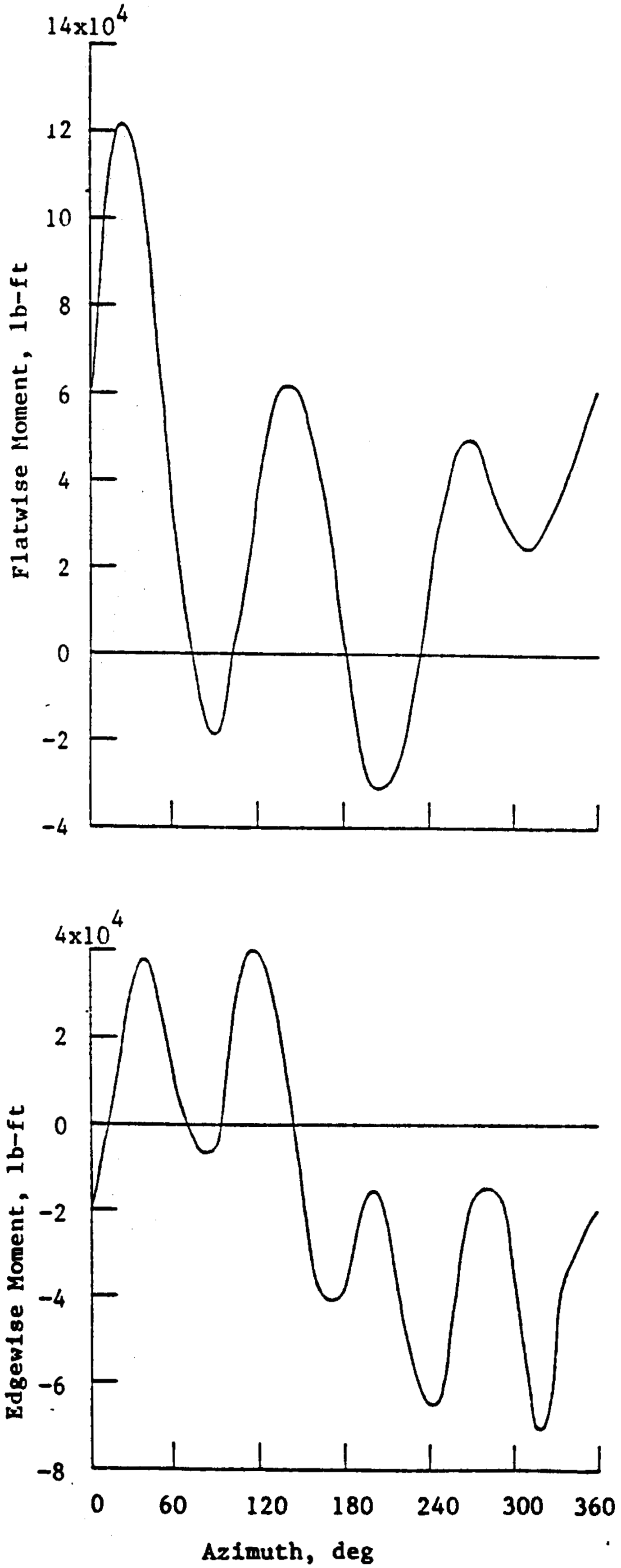

Figure 8. Time Histories of Blade Bending Loads: CASE I, Station 40

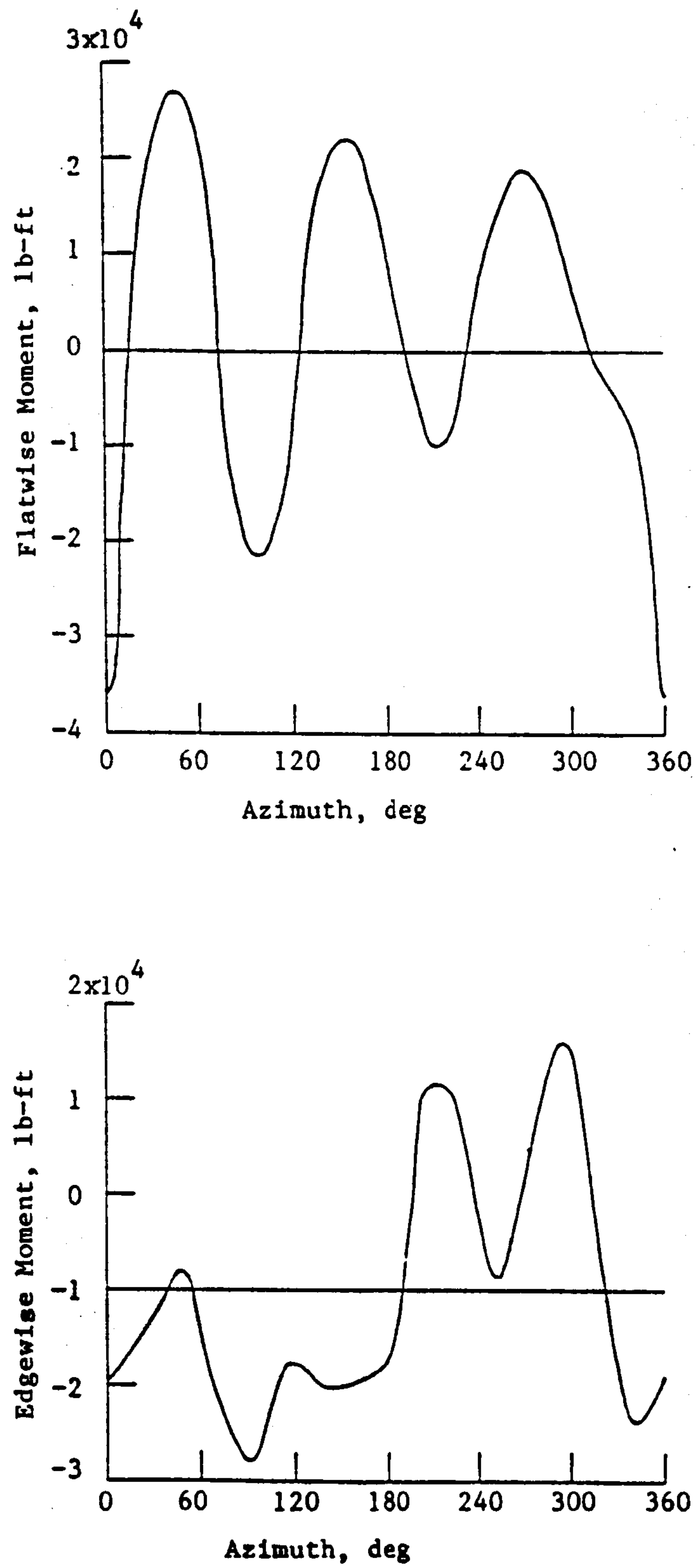

Figure 9. Time Histories of Blade Bending Loads: CASE I, Station 370

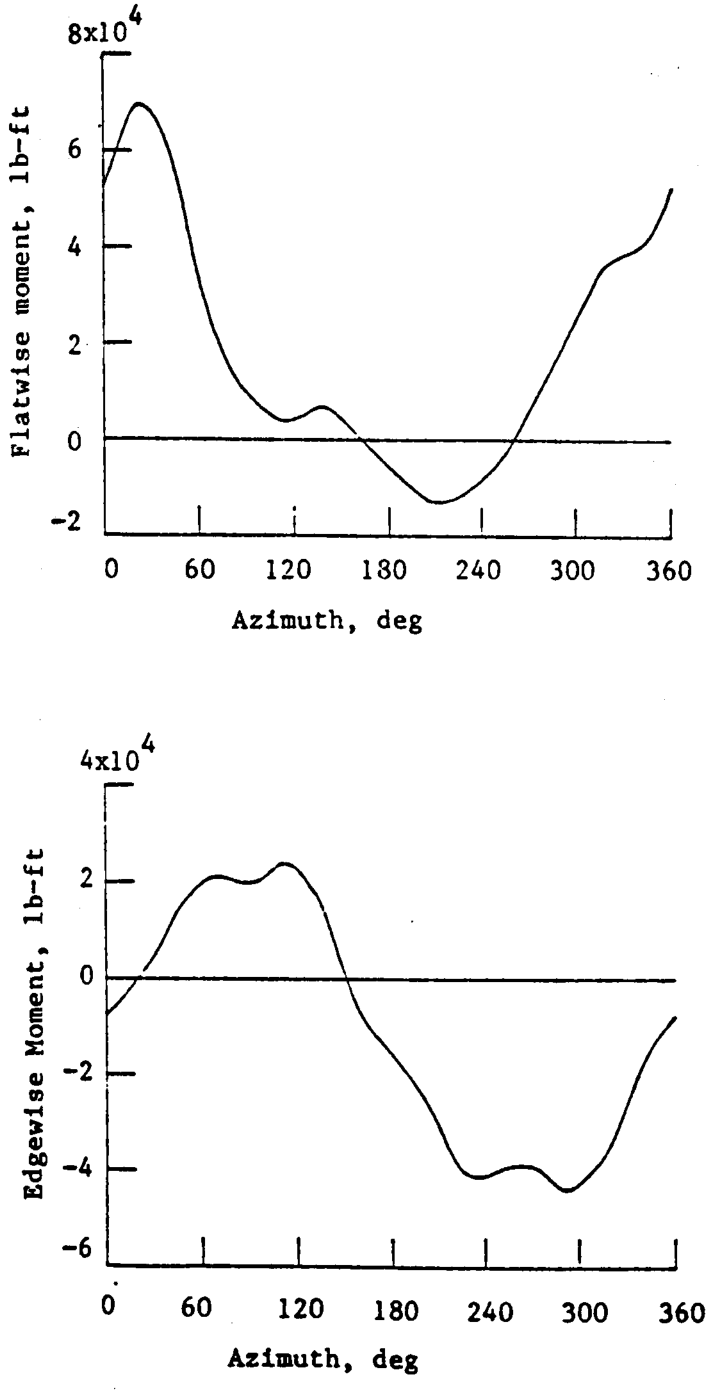

Figure 10. Time Histories of Blade Bending Loads: CASE IV, Station 40

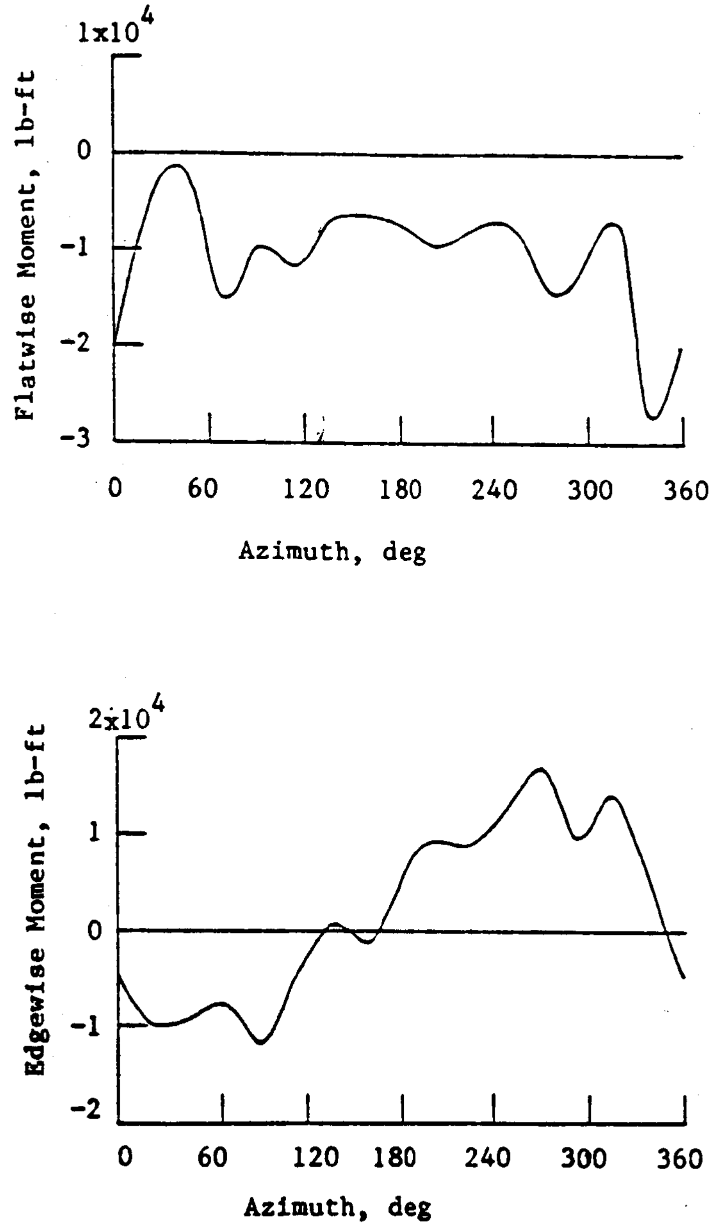

Figure 11. Time Histories of Blade Bending Loads: CASE IV, Station 370

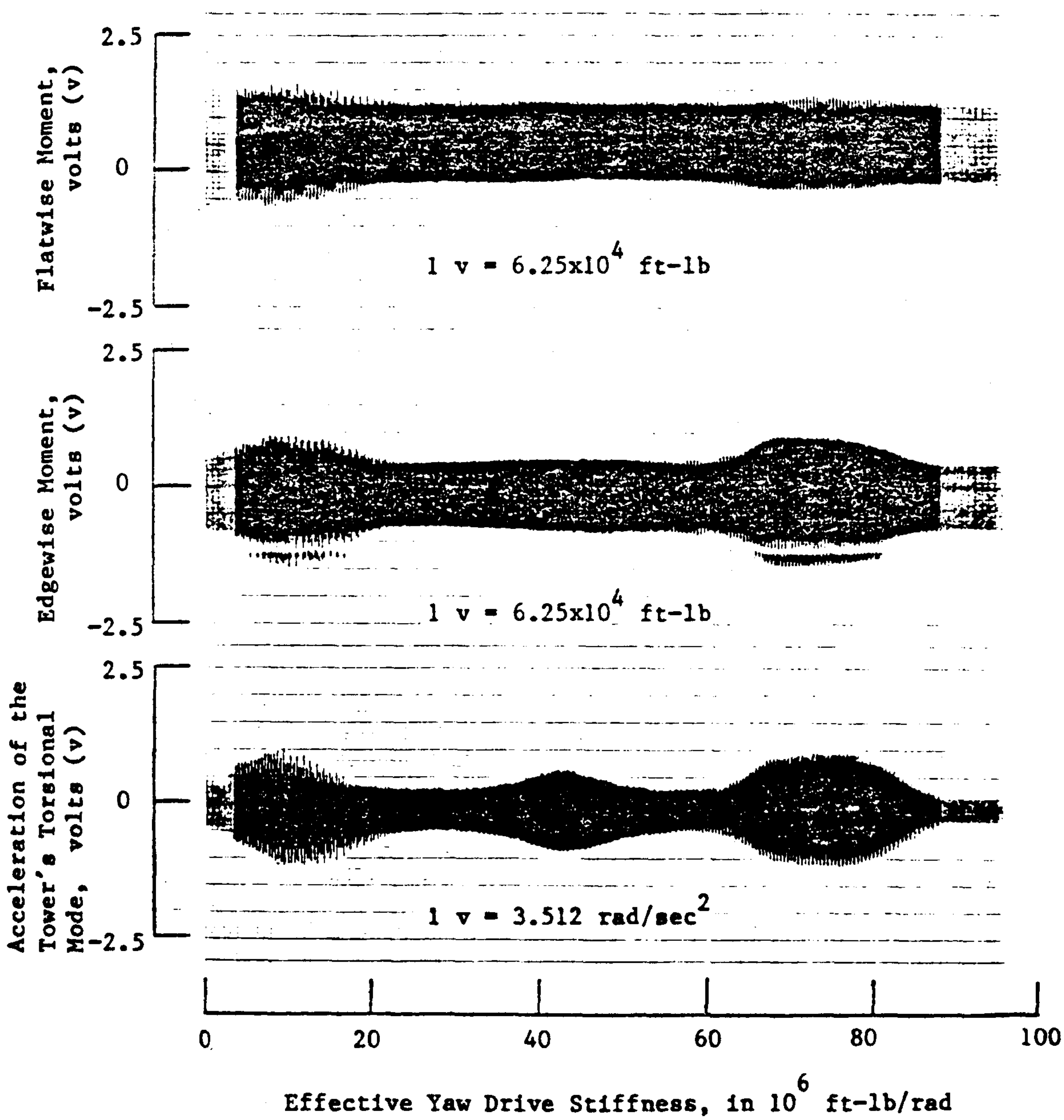

Figure 12. Influence of the Yaw Drive Stiffness on the Blade Bending Moments, and the Tower's Torsional response

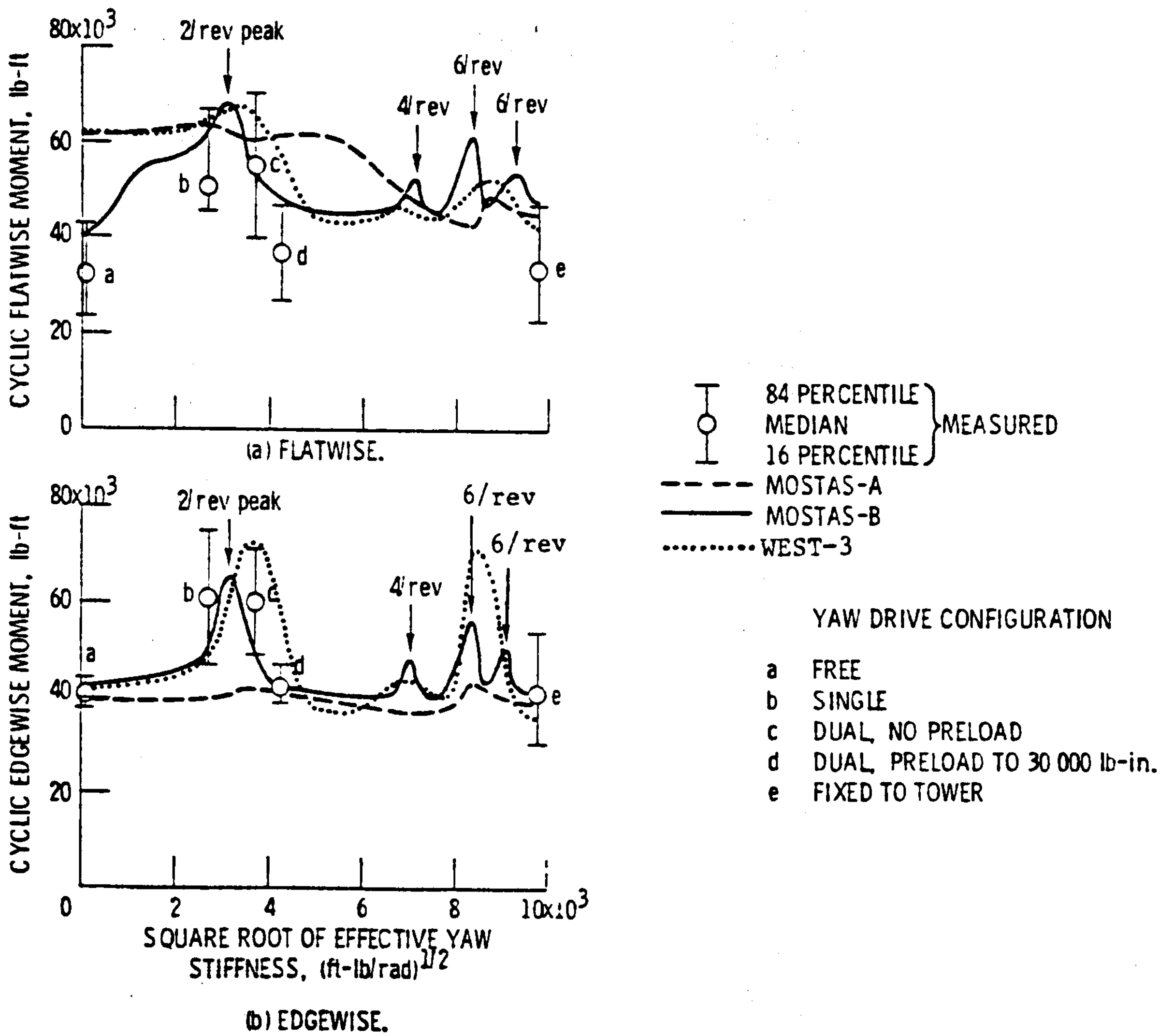

Figure 13. Blade Cyclic Bending Moments as Functions of the Square Root of Effective Stiffness of the Yaw Drive. (Station 40 Loads)

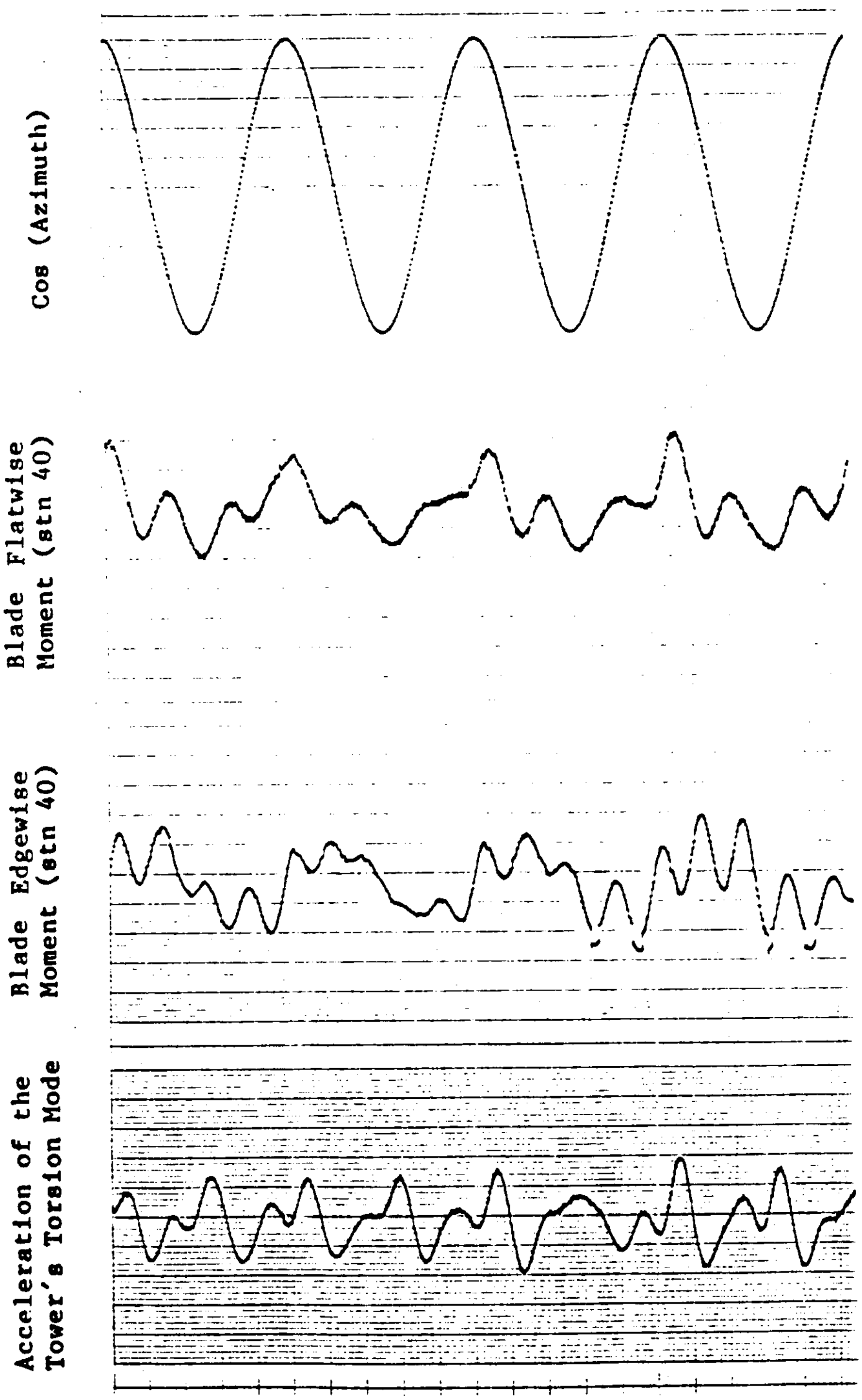

Figure 14. Responses for Yaw Drive Stiffness = 11.87×10^6 ft-lb/rad: 2/rev

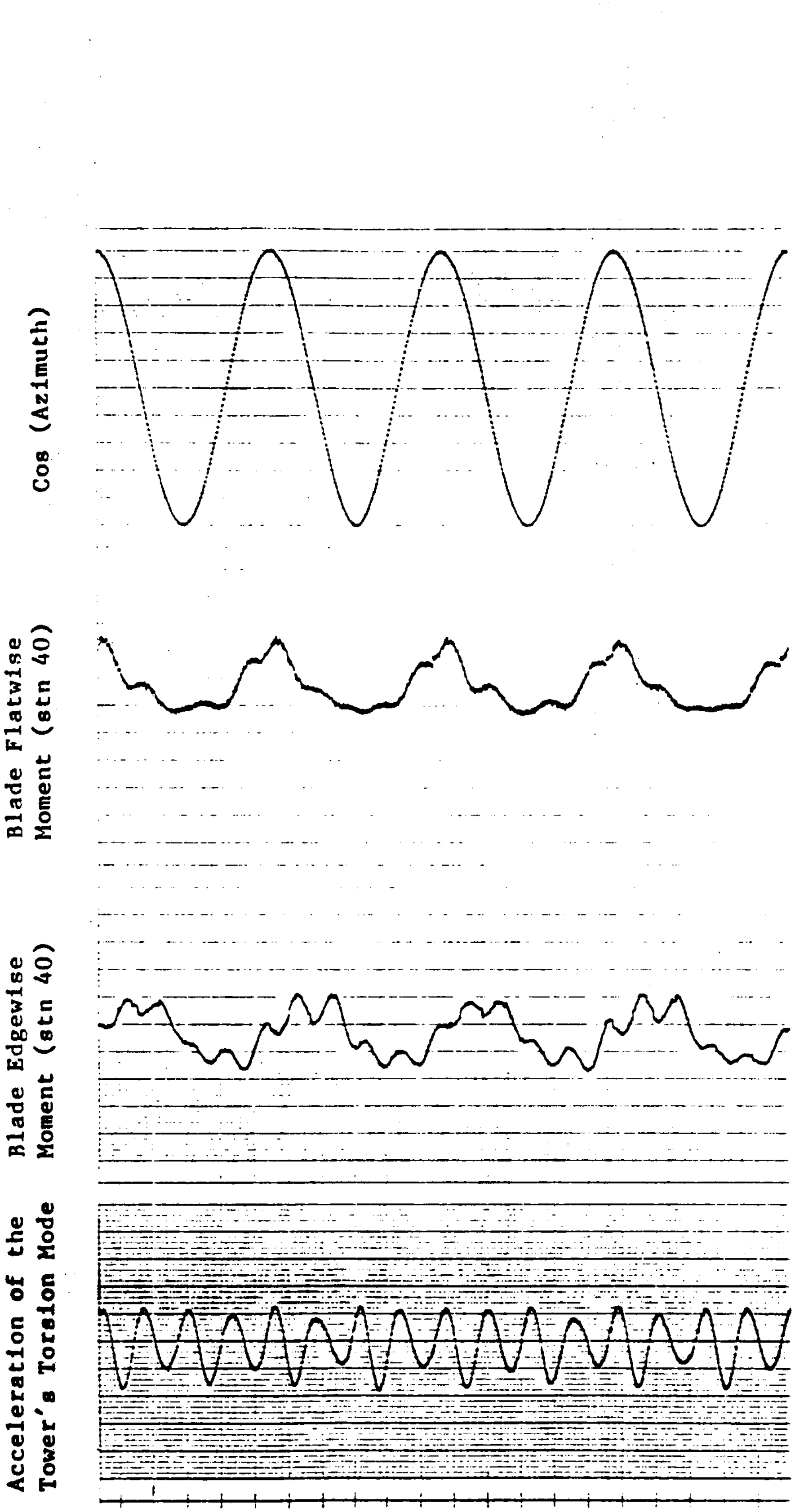

Figure 15. Responses for Yaw Drive Stiffness = 1.0×10^8 ft-lb/rad: 4/rev

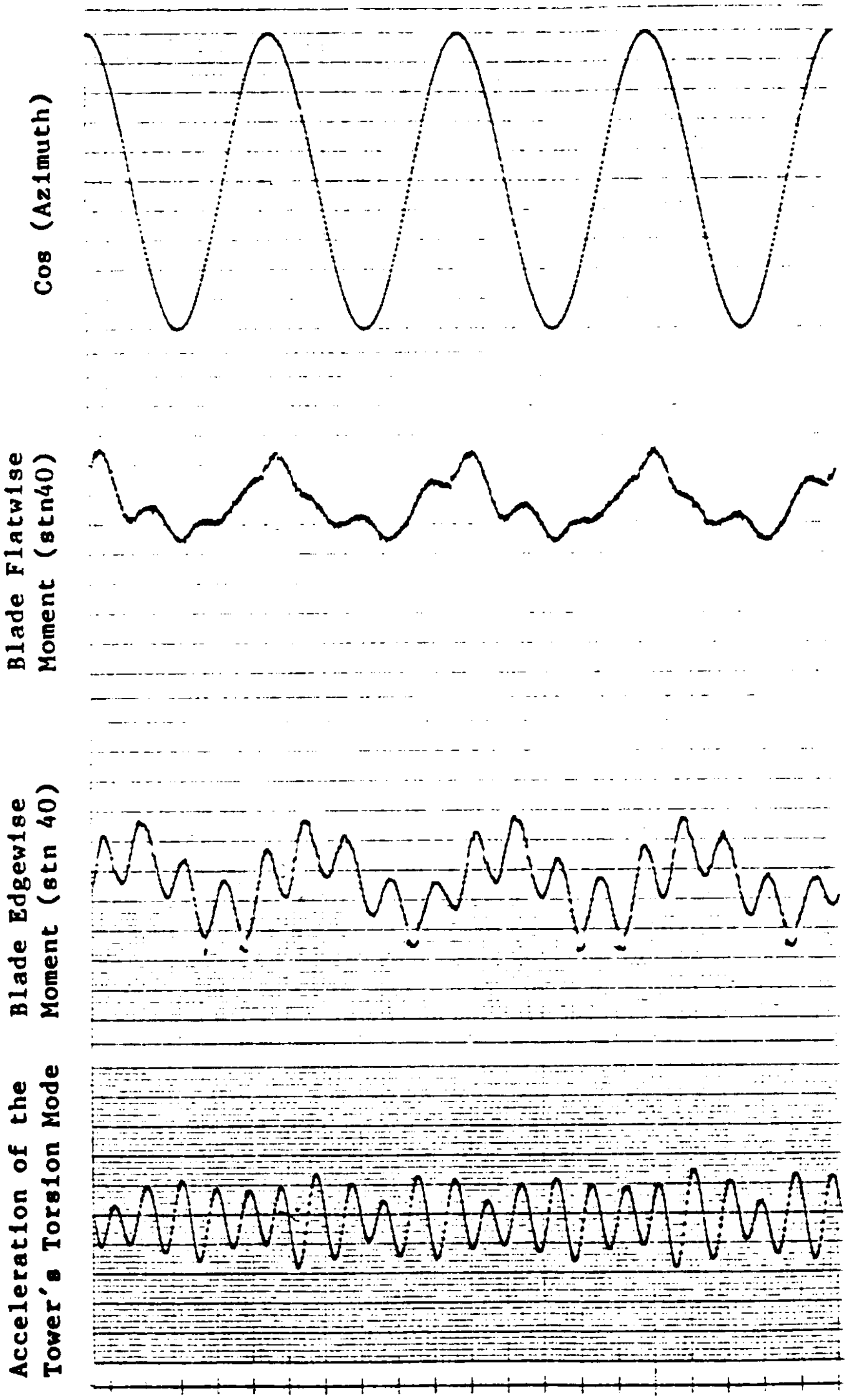

Figure 16. Responses for Yaw Drive Stiffness = $2.5x10^8$ ft-lb/rad: 6/rev

Table 1. Cyclic Bending Moments for Cases I and IV

Case	Source	Flatwise Moment, $\pm 10^3$ ft-lbs stn 40	Flatwise Moment, $\pm 10^3$ ft-lbs stn 370	Edgewise Moment, $\pm 10^3$ ft-lbs stn 40	Edgewise Moment, $\pm 10^3$ ft-lbs stn 370
I	Nominal Test Data	64.0	19.0	64.0	16.2
	MOSTAB-HFW	63.7	18.8	42.5	9.4
	WEST-2	58.6	45.0	39.0	13.3
	WEST-3	76.6	28.0	50.7	21.9
IV	Nominal Test Data	35.0	10.2	40.0	8.1
	MOSTAB-HFW	40.8	11.9	40.0	8.4
	WEST-2	34.7	14.7	37.6	21.9
	WEST-3	41.5	11.7	34.0	14.4

Table 2. Peak Bending Moments for Cases I and IV

Case	Source	Flatwise Moment, $\pm 10^3$ ft-lbs stn 40	Flatwise Moment, $\pm 10^3$ ft-lbs stn 370	Edgewise Moment, $\pm 10^3$ ft-lbs stn 40	Edgewise Moment, $\pm 10^3$ ft-lbs stn 370
I	Nominal Test Data	124.6	30.6	80.7	19.0
	MOSTAB-HFW	127.0	34.5	63.1	13.8
	WEST-2	118.7	65.0	54.6	18.3
	WEST-3	122.1	36.3	62.8	25.6
IV	Nominal Test Data	66.5	15.2	54.3	10.7
	MOSTAB-HFW	81.1	19.7	57.4	12.1
	WEST-2	75.0	25.2	58.0	25.6
	WEST-3	70.1	26.8	44.1	16.9

Table 3. Harmonic Bending Moments for Cases I and IV

CASE I

Stn	Harmonic number	Flatwise Moment, $\pm 10^3$ ft-lb			Edgewise Moment, $\pm 10^3$ ft-lb		
		Test Data	WEST-2	WEST-3	Test Data	WEST-2	WEST-3
40	1 P	31.2	30.3	31.0	42.5	38.4	33.7
	2 P	25.7	11.6	12.2	5.2	7.2	7.5
	3 P	17.4	18.3	42.5	11.6	2.7	12.8
	4 P	7.1	14.0	7.3	2.4	2.7	19.4
	5 P	7.8	-	7.2	13.8	-	15.3
	6 P	3.0	-	3.0	2.2	-	6.0
370	1 P	8.8	7.7	4.8	8.0	10.3	13.3
	2 P	6.2	5.4	3.1	2.2	4.1	5.2
	3 P	4.4	11.8	19.6	4.1	4.7	4.1
	4 P	1.1	11.1	8.1	0.4	3.4	9.8
	5 P	3.9	-	5.0	5.2	-	3.9
	6 P	0.7	-	3.9	0.4	-	1.9

CASE IV

Stn	Harmonic number	Flatwise Moment, $\pm 10^3$ ft-lb			Edgewise Moment, $\pm 10^3$ ft-lb		
		Test Data	WEST-2	WEST-3	Test Data	WEST-2	WEST-3
40	1 P	20.0	22.3	33.2	42.3	38.7	33.7
	2 P	9.8	6.9	8.7	1.5	2.6	1.5
	3 P	6.2	10.2	7.8	5.2	2.4	2.4
	4 P	3.5	6.5	4.3	3.6	0.8	0.6
	5 P	2.0	-	2.3	2.5	-	3.8
	6 P	0.7	-	4.4	0.4	-	6.3
370	1 P	6.2	2.4	3.8	7.1	20.0	12.1
	2 P	2.4	4.1	2.2	0.5	0.6	2.6
	3 P	1.8	5.2	3.5	1.4	0.6	0.9
	4 P	1.0	4.1	3.8	0.7	0.9	1.1
	5 P	0.6	-	3.9	0.7	-	2.3
	6 P	0.1	-	1.7	0.2	-	1.5

Table 4. Influence of Yaw Drive Stiffness on WEST-3 Cyclic Bending Moments

Case	Yaw Drive Stiffness, ft-lbs/rad	* Effective Stiffness, ft-lbs/rad	Cyclic Moments, $\pm 10^3$ ft-lb Flatwise	Edgewise	Remarks
1	0.0	0.0	62.5	40.6	Free yaw
2	2.25×10^6	2.20×10^6	62.5	43.8	Soft yaw
3	7.91×10^6	7.31×10^6	59.7	48.0	Single yaw drive
4	11.87×10^6	10.57×10^6	68.8	58.8	2/rev resonance
5	15.81×10^6	13.58×10^6	67.0	74.0	Dual yaw drive; no preload
6	22.35×10^6	18.14×10^6	58.0	65.0	Dual yaw drive; with preload
7	1.00×10^8	49.02×10^6	46.9	43.7	4/rev resonance
8	2.50×10^8	69.44×10^6	68.0	50.0	6/rev resonnce
9	8.60×10^8	86.48×10^6	47.0	42.0	6/rev resonance
10	1.00×10^{12}	96.14×10^6	43.8	37.5	Fixed yaw

* Combined with the tower stiffness of 96.15×10^6 ft-lbs/rad

1. Report No.	2. Government Accession No.	3. Recipient's Catalog No.
NASA CR-174982		

4. Title and Subtitle

WEST-3 Wind Turbine Simulator Development
Volume 2: Verification

5. Report Date

July 1985

6. Performing Organization Code

7. Author(s)

S. Sridhar

8. Performing Organization Report No.

PPI-FID-300102

10. Work Unit No.

9. Performing Organization Name and Address

Paragon Pacific Inc.
530 Maple Ave.
Torrance, California 90503

11. Contract or Grant No.

DEN 3-247

13. Type of Report and Period Covered

Contractor Report

12. Sponsoring Agency Name and Address

National Aeronautics and Space Administration
Washington, D.C. 20546

14. Sponsoring Agency ~~Code~~ Report No.

DOE/NASA/0247-2

15. Supplementary Notes

Final Report. Prepared under Interagency Agreement DE-AI01-76ET20320. Project Manger, D. Janetzke, Structures Division, NASA Lewis Research Center, Cleveland, Ohio 44135.

16. Abstract

The details of a study to validate WEST-3, a new real time wind turbine simulator developed by Paragon Pacific Inc., are presented in this report. For the validation, the MOD-0 wind turbine was simulated on WEST-3. The simulation results were compared with those obtained from previous MOD-0 simulations, and with test data measured during MOD-0 operations. The study was successful in achieving the major objective of proving that WEST-3 yields results which can be used to support a wind turbine development process. The blade bending moments, peak and cyclic, from the WEST-3 simulation correlate reasonably well with the available MOD-0 data. The simulation was also able to predict the resonance phenomena observed during MOD-0 operations.

Also presented in the report is a description and solution of a serious numerical instability problem encountered during the study. The problem was caused by the coupling of the rotor and the power train models.

The results of the study indicate that some parts of the existing WEST-3 simulation model may have to be refined for future work; specifically, the aerodynamics, and the procedure used to couple the rotor model with the tower and the power train models.

17. Key Words (Suggested by Author(s))	18. Distribution Statement
Wind turbine simulation Parallel processing	Unclassified - unlimited STAR Category 44 DOE Category UC-60

19. Security Classif. (of this report)	20. Security Classif. (of this page)	21. No. of pages	22. Price*
Unclassified	Unclassified	28	A03

*For sale by the National Technical Information Service, Springfield, Virginia 22161